Velocity-space pictures of continuum electrons produced by slow, bare, highly charged ions

M. Abdallah,[1] S. Kravis,[1,*] C. L. Cocke,[1] Y. Wang,[2] V. D. Rodriguez,[3] and M. Stöckli[1]
[1]*J. R. Macdonald Laboratory, Physics Department, Kansas State University, Manhattan, Kansas 66506-2604*
[2]*Pacific Bell, 2600 Camino Ramon, IE800B, San Ramon, California 94583*
[3]*Departmento de Fisica, Universidad de Buenos Aires, 1428 Buenos Aires, Argentina*
(Received 6 December 1996; revised manuscript received 8 May 1997)

Velocity-space pictures of the electron continua produced by the impact of ions on He and Ne have been measured for the bare projectiles of p, He, C, O, and Ne at a projectile velocity of 1.63 a.u. For the three highly charged projectiles, this velocity lies in the ionization ''threshold'' region where electron capture dominates the reaction. The electron velocity-space distributions for these cases are concentrated near the velocity of the projectile, not near the saddle-point velocity, and seem to ''saturate'' at a nearly universal shape. The data are in qualitative agreement with CDW-EIS calculations. [S1050-2947(97)08909-9]

PACS number(s): 34.50.Fa, 39.30.+w

I. INTRODUCTION

The production of continuum electrons in the collision of slow, bare, highly charged ions with light targets (in this case, He) has been the object of discussion for more than a decade. Highly charged ions with velocities very much below that of the target electrons tend to capture electrons from the target into bound states on the projectile, and only rarely leave them in the continuum. It was suggested by Olson [1] that electrons removed from the target could escape capture if they are stranded on the saddle in the potential formed by the two receding positively charged ions. The physical picture is reminiscient of near-threshold Wannier [2] ionization, and, indeed, continuum electron production via collisions in this low energy has many features in common with threshold photon and electron impact ionization. Olson's suggestion was supported by both classical trajectory Monte Carlo (CTMC) and coupled channel calculations [3,4]. Experimental evidence for ''saddle-point'' electrons was reported by Olson *et al.* [5]. Considerable controversy followed, with subsequent experiments both supporting [6–8] and disagreeing with [9–14] this identification. A common theme of the experimental papers has been the effort to confirm or deny the importance of saddle-point electrons by asking whether the continuum electron energy spectra display a maximum at the velocity, v_s, with which the saddle moves asymptotically ($v_s = v_p/[1+\sqrt{q_p/q_t}]$), where v_p is the projectile velocity and q_p and q_t are projectile and final target charges, respectively) and whether this maximum moves appropriately with changes in q_p.

Several problems have contributed to the confusion surrounding the identification of a saddle-point feature. Most previous experiments have been carried out at a single laboratory angle, from which it is difficult to see a comprehensive picture of the electron velocity-space distribution. Experiments carried out with nonbare projectiles are complicated by intersystem electron-electron interactions [14]. Finally, experiments seeking the saddle-point feature should ideally be carried out in the so-called threshold velocity region. This region does not simply correspond to the matching of the projectile velocity with the target electron velocity, as might be expected. As discussed in Refs. [15–17], the projectile velocity at which electron capture ceases to dominate direct ionization is dependent on the projectile charge, and is given approximately by $v_{\min} = q_p^{1/4} I^{1/2}$, where I is the target ionization potential in a.u. and q_p the projectile charge. Thus the threshold velocity region corresponds to velocities $v < v_{\min}$. For large q_p, velocities above 1 a.u. can thus be low velocities when judged by this criterion. Most experiments, especially those with multiply charged projectiles, have used higher velocity projectiles.

This paper reports comprehensive velocity-space pictures of soft electron spectra produced by the impact of slow, bare ions of p, He, C, O, and Ne on He and Ne. An earlier paper has presented similar velocity-space imaging data for bare C and protons on He, and we include some of those data here for completeness. In this paper we focus specifically on the question of saddle-point electrons for highly charged projectiles, and present data for a single velocity but over a wide range of projectile charges and for two different targets. (A brief account of some of the present results are in Ref. [18].) The experiment avoids the problems listed above in that comprehensive velocity-space spectra are measured for *all* laboratory angles, only bare projectiles are used and, for the three higher charged ions, the velocities are well below $v_{\min}$. This last criterion is not met for the p and He^{2+} data, and those data are included here only for comparison. For the three most highly charged projectiles, the results show clearly that no saddle-point ''feature'' can be identified from the comprehensive velocity space distributions of the continuum electrons. Indeed, the spectra for these three projectiles seem to ''saturate'' at a nearly universal spectral shape centered much nearer to the velocity of the projectile than that of the saddle. For the two lighter projectiles considerable population in the saddle region is seen, but it is perhaps a matter of semantics whether these are to be called saddle-point electrons, since the major spectral feature does not vary with projectile charge as would be expected for a saddle-point feature.

Part of our motivation for performing the experiment for

*Present address: NOVA R&D, 1525 Third St., Riverside, CA 92507.

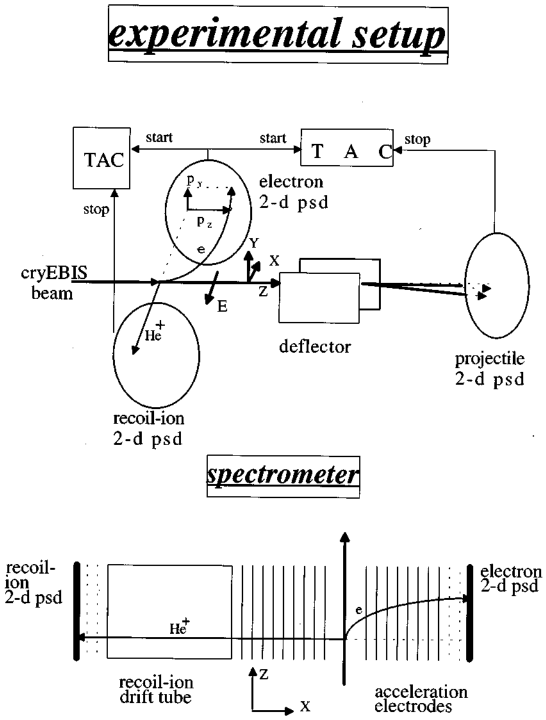

FIG. 1. Schematic of apparatus used.

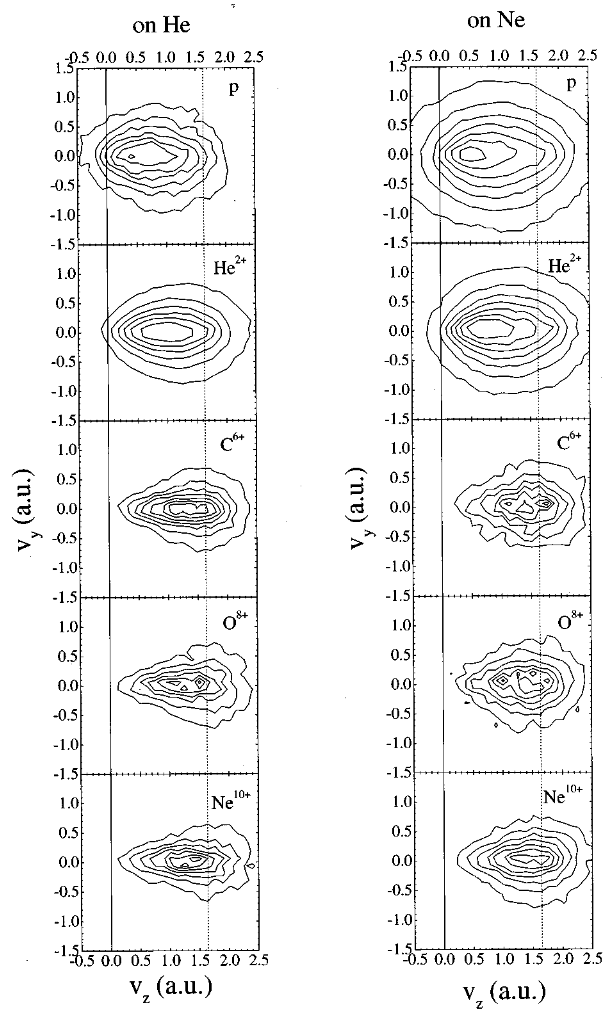

FIG. 2. Two-dimensional plots of the velocity-space continuum electron distributions, projected into the v_z-v_y plane, for various bare projectiles on He and Ne at $v_p = 1.63$ a.u. The solid and dashed lines locate $v=0$ and $v=v_p$, respectively.

the three highly charged ions in this low velocity region is that two definite ''mechanisms,'' have been proposed for ionization in this region, based on theoretical treatments [19–26]. These are the ''*S*'' and ''*T*'' processes discussed by many authors, and especially addressed in the language of hidden crossings. The *T* process, which corresponds to a saddle-point mechanism, is expected to leave electrons centered near v_s [22,26]. The *S* process, which promotes electrons directly into the molecular continuum at small internuclear distances, is expected to leave the electrons near the velocity of the center of mass of the system. For heavy, highly charged projectiles, this means near v_p. Both total cross sections [26,27] and electron continua have been evaluated for these processes for *p* on H using hidden-crossing techniques. The only continuum electron measurement carried out in the threshold region seems to be that of Pieksma [28] for *p* on H, which showed a total energy spectrum consistent with that expected for *T* process electrons. Doerner *et al.* [30] have recently presented electron continua showing evidence for saddle-point electrons for *p* on He above 5 keV. For bare, highly charged projectiles, only total cross sections have previously appeared [15,29]. No quantitative theoretical evaluation of the expected electron continua for *S* and *T* processes, or any other coupled channel calculation for the continuum spectrum, has appeared for a He target.

II. EXPERIMENTAL TECHNIQUE

The velocity-space distributions were measured using the experimental apparatus discussed in Ref. [31] and reproduced in Fig. 1 for convenience. The beam from the Kansas State University EBIS passed through a collision region filled with He or Ne gas at a pressure of a few times 10^{-6} mbar, where it both captured and ionized the target. A transverse electric field of 420 V/cm transported the He ions onto the face of a two-dimensional position-sensitive channel-plate detector (PSD). In this strong field, each He ion travels nearly in a straight line, and provides the y-z coordinates of the position at which the reaction occurred (see Fig. 1 for coordinate system). The ion flight time was also recorded to identify its charged state. The electron was projected the other way onto a second PSD, where its position of arrival in the y-z plane, relative to that of the ion, was used to calculate the y and z components of the velocity with which the electron departed the reaction. This calculation relies on knowing the flight time of the electrons to this detector, which is calculated on the assumption that the transverse velocity (v_x) of the electron is small. This turns out to be a very good assumption, as the experimental results show that v_x is typically below 0.5 a.u., corresponding to transverse energies below 3 eV. A triple coincidence measurement was performed (electron, He ion, and charge-state analyzed projectile) to identify collisions in which a single electron, a He^+ ion and a bare projectile exited the reaction.

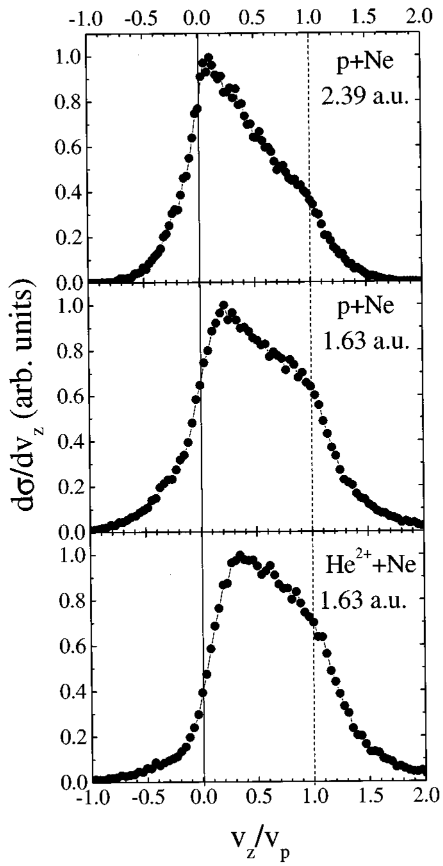

FIG. 3. Slices of three velocity-space distributions for Ne for $|v_y|<0.1$ a.u., projected onto the v_z axis. The kinks at $v=v_p$ are due to cusp electron production.

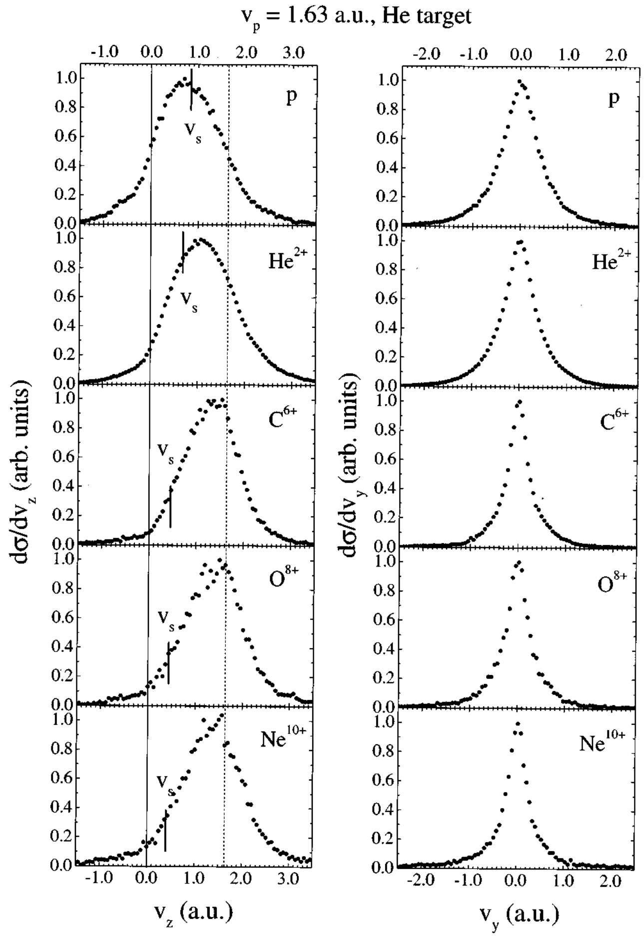

FIG. 4. Projections of the data of Fig. 2, for the He target, onto (a) the longitudinal (v_z) and (b) transverse (v_y) axes. The saddle point velocity is denoted as v_s.

Other final channels were also recorded and used to perform control checks on the electron velocity calibration, but are not the point of this paper.

The electron velocity spectrum so obtained corresponds to the projection of the full velocity-space distribution onto the y-z plane. Since the collision has cylindrical symmetry about the z axis (no collision plane is determined in this experiment), this is sufficient to uniquely determine the electron velocity-space spectrum, although no attempt to unfold a ''radial'' transverse electron momentum spectrum has been made. Similar momentum-imaging techniques for electrons have been used by several previous authors [31–34] and are commonly used for recoil ions [35]. The more complete measurement by Doerner *et al.* [30] for p on He extends this technique to determine the collision plane and recoil momentum as well. For the electric fields used here, electrons with longitidunal momenta up to 2 a.u. (54 eV) were covered without loss.

III. RESULTS AND DISCUSSION

Figure 2 shows contour pictures of the velocity-space y-z spectra for the five projectiles. These spectra represent $d\sigma^3/d\vec{v}$, integrated over v_x. The vertical lines indicate the positions of the target-centered ($v=0$) and projectile-centered ($v=v_p$) continua. For proton bombardment, for which 1.63 a.u. is already near velocity matching, the spectrum is seen to have considerable population in the center between the two velocities, or in the vicinity of the saddle of the asymptotic final potential. As the projectile charge is raised the spectrum narrows in the transverse direction to focus onto the z axis. In the longitidunal direction, the center moves nearer the projectile velocity. This is just opposite to the way the velocity of the asymptotic saddle point moves as q_p increases.

Figure 3 shows projections from the spectra of Fig. 2 corresponding to slices in v_y near the beam axis ($|v_y|<0.2$ a.u.). Such a projection enhances features that dominate only for small transverse momentum. In particular, the ''cusp'' peak, which appears routinely as a strong feature in electron spectra taken at zero degrees, is seen in these projections as a ''kink'' in the spectra at a velocity equal to the projectile velocity. The cusp feature is weak in our presentation because we are integrating over the x component of momentum, which tends to deemphasize sharp features, and because we are presenting the entire cross section picture, on a linear scale, and the cusp peak is a very weak contributor to the total cross section for these collisions. This peak is also somewhat attenuated by the finite resolution of the present experiment, which is discussed in detail in Ref. [29]. Since that discussion is rather complete and involved we choose not to repeat it here. For the present cases, the fractional

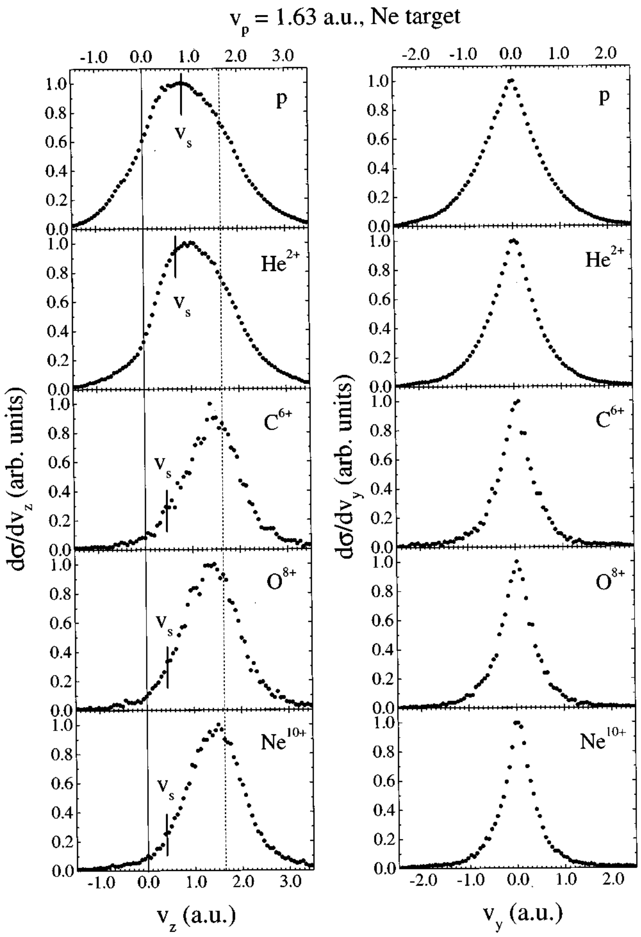

FIG. 5. Projections of the data of Fig. 2, for the Ne target, onto (a) the longitidunal (v_z) and (b) transverse (v_y) axes. The saddle point velocity is denoted as v_s.

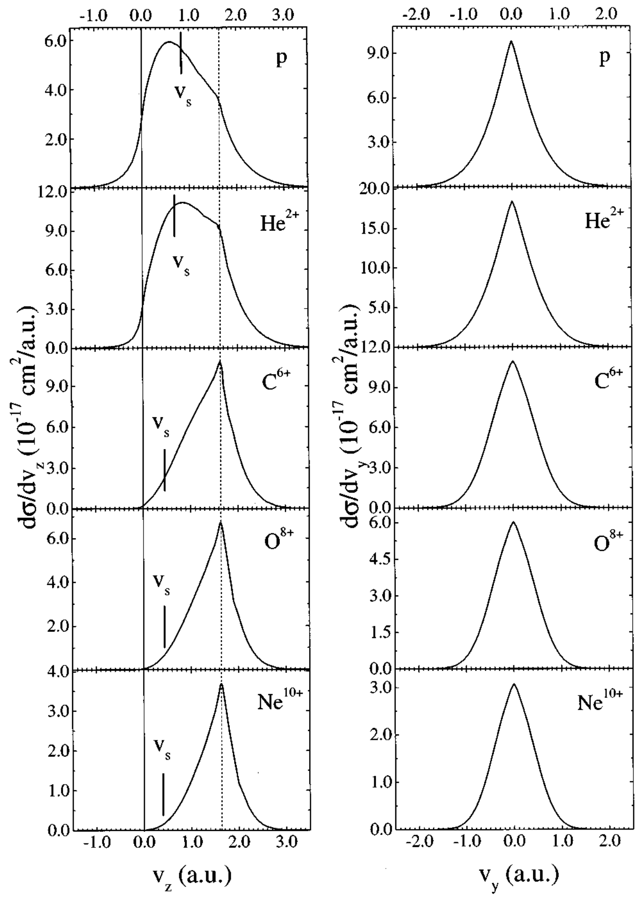

FIG. 6. Theoretical CDW-EIS calculations of the transverse and longitidunal velocity distributions for the He target. These distributions are to be compared to the data of Fig. 4.

momentum resolution is typically between 4 and 8% in v_z, and below 8% in v_y. To each of these should be added an absolute resolution contribution of approximately 0.1 a.u. The appearance of the kink at the velocity of the projectile serves as confirmation of the correct calibration of the z-velocity scale. Our spectra are qualitatively very similar to those of Vanjai *et al.* [36], who measured the projectile energy loss spectrum for ionization of He by protons.

Total projections of the spectra of Fig. 2 onto the longitidunal (v_z) and transverse (v_y) axes are shown in Figs. 4 and 5. These spectra have been normalized to the same peak height in this figure. The shapes of the longitudinal spectra are seen to ''saturate'' at a nearly universal shape for the three highest charged projectiles. While it is expected that the projectile potential dominates the motion of the electrons for such a collision system, it is less obvious that the continuum electrons will so closely accompany the projectile in velocity space, since they are easily captured into bound states if they end up spatially located near the projectile.

In Fig. 6 we show a continuum-distorted-wave-eikonal-initial-state (CDW-EIS) [37,38] calculation for He, which qualitatively reproduces the saturation effect and the centering of the continuum on the projectile. The calculation also reproduces qualitatively the narrowing of the distributions in the transverse direction. We note that this calculation is being applied rather outside its expected range of validity, and produces both cross sections that are too high in this region and spectra that are too sharply peaked on the projectile. It has been previously noted by McCartney [39] that CDW-EIS provides no evidence for saddle-point features for several projectiles on H. We have no quantitative evaluation of *S* and *T* process predictions for such asymmetrical systems. It is clear that that no dominance of saddle-point electrons near v_s, to be associated with the *T* process, is to be found in the experimental data. It remains to be determined from calculations whether the *T* process really predicts such a feature for such systems.

IV. SUMMARY AND CONCLUSIONS

In summary, we have presented velocity-space pictures of the electron continua produced by 1.63 a.u. *p*, He, C, O, and Ne bare projectiles on He. The spectra are quite focused along the beam axis for the three highly charged projectiles, but show no sign of centering about the saddle-point velocity except for the proton-projectile case. Instead, the projectile spectra tend to saturate at a nearly universal shape centered near the projectile velocity as the projectile charge is raised.

This feature is qualitatively, but not quantitatively, reproduced by CDW-EIS calculations. In spite of the many years of effort that have been dedicated to understanding continuum electron production in simple collisions sytems, there seems as yet to be no theoretical calculation which provides a fully successful quantitative treatment of the process of low energy ionization by highly charged ions.

ACKNOWLEDGMENTS

The authors are grateful to R. Doerner, M. Pieksma, R. E. Olson, S. Ovchinnikov, and J. Macek for stimulating conversations concerning this subject. This work was supported by the Division of Chemical Sciences, Office of Basic Energy Systems, Office of Energy Research, U.S. Department of Energy.

[1] R. E. Olson, Phys. Rev. A **27**, 1871 (1983).
[2] G. H. Wannier, Phys. Rev. **90**, 817 (1953).
[3] R. Shakeshaft, Phys. Rev. A **18**, 1930 (1978).
[4] T. G. Winter and C. D. Lin, Phys. Rev. A **29**, 3071 (1984).
[5] R. E. Olson, T. J. Gay, H. G. Berry, E. B. Hale, and V. D. Irby, Phys. Rev. Lett. **59**, 36 (1987).
[6] V. D. Irby *et al.*, Phys. Rev. A **37**, 3612 (1988).
[7] T. J. Gay, M. W. Gealy, and M. E. Rudd, J. Phys. B **23**, L823 (1990).
[8] V. D. Irby, S. Datz, P. Dittner, N. Jones, H. F. Krause, and C. R. Vane, Phys. Rev. A **47**, 2957 (1993).
[9] R. D. Dubois, Phys. Rev. A **48**, 1123 (1993).
[10] W. Meckbach, S. Suarez, P. Focke, and G. Bernardi, J. Phys. B **24**, 3763 (1991).
[11] G. Bernardi, S. Suarez, P. Fainstein, C. Garibotti, W. Meckbach, and P. Focke, J. Phys. B **23**, L829 (1990).
[12] G. Bernardi, P. Fainstain, C. R. Garibotti, and S. Suarez, J. Phys. B **23**, L139 (1990).
[13] G. Bernardi *et al.*, Phys. Rev. A **40**, 6863 (1989).
[14] R. D. Dubois, Phys. Rev. A **50**, 364 (1994).
[15] W. Wu, C. L. Cocke, J. P. Giese, F. Melchert, M. Rapahelian, and M. Stöckli, Phys. Rev. Lett. **75**, 1054 (1995).
[16] N. Bohr, K. Dan. Vidensk. Selsk. Mat. Fys. Medd. **18**, 8 (1948).
[17] N. Bohr and J. Lindhard, K. Dan. Vidensk. Selsk. Mat. Fys. Medd. **128**, 7 (1954).
[18] M. Abdallah *et al.*, Phys. Scr. (to be published).
[19] S. Yu. Ovchinnikov and E. A. Solo'ev, Zh. Eksp. Teor. Fiz. **90**, 921 (1986) [Sov. Phys. JETP **63**, 538 (1986)].
[20] E. A. Solov'ev, Zh. Eksp. Teor. Fiz. **81**, 1681 (1981) [Sov. Phys. JETP **54**, 893 (1981)].
[21] S. Yu. Ovchinnikov and E. A. Solov'ev, Comments At. Mol. Phys. **22**, 69 (1988).
[22] A. Barany and S. Yu. Ovchinnikov, Phys. Scr. **46**, 243 (1993).
[23] J. E. Macek and S. Yu. Ovchinnikov, Phys. Rev. A **50**, 468 (1994).
[24] P. S. Krstic and R. K. Janev, Phys. Rev. A **47**, 3894 (1993).
[25] R. K. Janev, G. Ivanovski, and E. A. Solov'ev, Phys. Rev. A **49**, R645 (1994).
[26] S. Yu. Ovchinnikov and J. Macek, Phys. Rev. Lett. **75**, 2474 (1995).
[27] M. Pieksma and S. Yu. Ovchinnikov, J. Phys. B **27**, 4573 (1994).
[28] M. Pieksma *et al.*, Phys. Rev. Lett. **73**, 3166 (1994).
[29] W. Wu *et al.*, Phys. Rev. A **53**, 2367 (1996).
[30] R. Doerner *et al.*, Phys. Rev. Lett. **77**, 4520 (1996).
[31] S. Kravis *et al.*, Phys. Rev. A **54**, 1394 (1996).
[32] R. Moshammer *et al.*, Phys. Rev. Lett. **73**, 3371 (1994).
[33] R. Moshammer *et al.*, Nucl. Instrum. Methods Phys. Res. B **108**, 425 (1996).
[34] H. Helm *et al.*, Phys. Rev. Lett. **70**, 3221 (1993).
[35] J. Ullrich *et al.*, Comments At. Mol. Phys. **30**, 285 (1994).
[36] T. Vanjai *et al.*, Phys. Rev. A **74**, 3588 (1995).
[37] D. S. F. Crothers and J. F. McCann, J. Phys. B **16**, 3239 (1983).
[38] P. D. Fainstein, V. H. Ponce, and R. D. Rivarola, J. Phys. B **24**, 3091 (1991).
[39] M. McCartney, Phys. Rev. A **52**, 1213 (1995).